N-cadherin expression level modulates integrin-mediated polarity and strongly impacts on the speed and directionality of glial cell migration

Emeline Camand[1], Florent Peglion[1], Naël Osmani[1,*], Marc Sanson[2,3] and Sandrine Etienne-Manneville[1,‡]

[1]Institut Pasteur–CNRS URA 2582, Cell Polarity, Migration and Cancer Unit, 25 rue du Dr Roux, 75724 Paris CEDEX 15, France
[2]UMR975, Hôpital de la Salpêtrière, Université Pierre et Marie Curie, Paris, 75013 France
[3]Service de Neurologie Mazarin, Hôpital de la Salpêtrière, Paris, 75013 France

*Present address: Institut de Génétique et de Biologie Moléculaire et Cellulaire, 1 rue Laurent Fries, 67404 Illkirch CEDEX, France
‡Author for correspondence (sandrine.etienne-manneville@pasteur.fr)

Accepted 23 September 2011
Journal of Cell Science 125, 844–857

doi: 10.1242/jcs.087668

Summary

Perturbation of cell polarity is a hallmark of cancer cells. In carcinomas, loss of epithelial E-cadherin contributes to the loss of cell polarity and promotes epithelial–mesenchymal transition and carcinoma infiltration. However, the contribution of classical cadherins to the development of non-epithelial tumours is less well documented. We investigated the impact of the level of N-cadherin expression on the polarity and migration of normal and tumour glial cells. Low levels of N-cadherin were frequently observed in human glioma samples and purified glioma cells. Using a wound-healing assay, we show that a decreased level of N-cadherin promotes a faster and less-directed migration both in normal and tumour cells. N-cadherin-mediated contacts control cell velocity and polarity through the regulation of focal adhesions. In cells expressing low levels of N-cadherin, small focal adhesions are present at the entire cell periphery of confluent cells and are not affected by wounding of the cell monolayer. Under these conditions, wound-induced integrin-mediated recruitment of the small GTPase Cdc42, activation of the Cdc42-mediated polarity pathway and centrosome reorientation do not occur. Re-expression of N-cadherin in gliomas restores cell polarity and strongly reduces cell velocity, suggesting that loss of N-cadherin could contribute to the invasive capacity of tumour astrocytes.

Key words: N-cadherin, Astrocyte, Glioma, Cell migration, Cell polarity

Introduction

Malignant gliomas are the most common and lethal primary intracerebral tumours in adults. They comprise a group of different kinds of tumours arising within the central nervous system and sharing characteristics with glial cells, namely astrocytes, oligodendrocytes or their precursors (Jung et al., 2010; Nishiyama et al., 1989; Prestegarden et al., 2010). Gliomas are currently classified by the World Health Organization (WHO) into four grades, where grade I comprises benign tumours and grade IV are the highly malignant tumours, also called glioblastomas, that are the most frequent (Kleihues et al., 1993; Louis et al., 2007). Glioblastomas are characterized by extensive genetic alterations, frequently including amplification of the gene encoding the epidermal growth factor receptor (EGFR) and loss of phosphatase and tensin homologue deleted on chromosome 10 (PTEN) activity, both promoting invasion (McLendon et al., 2008). While systemic metastases are rare, these cancers show an aggressive progression, characterized by widespread invasion throughout the brain parenchyma and resistance to classical therapeutic approaches (Giese, 2003). As a consequence, one major challenge is to prevent cell detachment and tumour spreading from the original tumour site.

Cell surface adhesion molecules are the principal mediators of interaction between cells and are thus likely to be key players in tumour spreading. Classical cadherins are Ca^{2+}-dependent transmembrane cell-adhesion molecules, which mediate homophilic interaction between adjacent cells and display tissue-specific expression (Angst et al., 2001; Takeichi, 1990). E-cadherin and N-cadherin are the best studied of these molecules and are, respectively, mainly expressed in epithelial and neural tissues (Hatta and Takeichi, 1986). Defects in the expression or function of cadherins have been implicated in carcinoma progression and metastasis (Makrilia et al., 2009). Loss of E-cadherin is observed, most often associated with an up-regulation of N-cadherin, which has, in this situation, a pro-migratory effect (Hazan et al., 2004). In gliomas, no obvious scenario has emerged on the basis of N-cadherin protein levels, and the role of N-cadherin in glioma cell migration is still unknown (Asano et al., 2004; Asano et al., 2000; Foty and Steinberg, 2004; Hegedus et al., 2006; Shinoura et al., 1995; Utsuki et al., 2002). We have recently shown that N-cadherin is a key regulator in the polarity of non-migrating astrocytes (Dupin et al., 2009). As loss of cell polarity is a common characteristic of tumour cells, we wondered whether alteration of N-cadherin levels in gliomas impacts on polarity and migration, a fundamentally polarized process.

To investigate how N-cadherin-mediated junctions could modulate cell migration, we used an in vitro wound-healing assay that induces a collective, directed migration (Etienne-Manneville and Hall, 2001; Faber-Elman et al., 1996; Nobes and

Journal of Cell Science

Hall, 1999). In this model, we and others have shown that primary astrocytes undergo a highly polarized migration, perpendicularly oriented to the scratch (Etienne-Manneville and Hall, 2001; Peng et al., 2008). Astrocyte polarization and migration are initiated by integrin engagement with the extracellular matrix at the wound edge of the cell. We show here that glioblastoma cells are unable to polarize and display a faster and less-directed migration in this assay. We also demonstrate that N-cadherin-mediated junctions contribute to the polarization and directed migration of astrocytes and that decreased N-cadherin expression is, at least partly, responsible for the abnormal migratory behaviour of glioblastoma cells. We attribute this role of N-cadherin to its regulatory function on focal adhesions and to the subsequent alteration of the integrin-dependent Cdc42 activity and polarity pathway. Our work broadens the role of N-cadherin in cell polarity and supports the idea that a decrease in N-cadherin levels contributes to the invasive capacity of astrocytic tumours.

Results

N-cadherin protein levels are often downregulated in glioma cells

Although sometimes contradictory, evidence showing changes in N-cadherin levels in gliomas is accumulating (Asano et al., 2004; Asano et al., 1997; Utsuki et al., 2002). We analyzed N-cadherin levels in normal and glioma samples by western blots. Quantitative western blotting comparing normal brain samples and high-grade gliomas showed a significant twofold decrease in N-cadherin expression in glioblastomas (Fig. 1A,B). To confirm the decrease in N-cadherin expression, we used purified tumour cells from tumour samples (G3-1, G4-1 and G4-2), as well as two different cell lines derived from human gliomas of different grades, the U138 (glioblastoma) and the U373 (astrocytoma, grade III) cells (Ponten and Macintyre, 1968). N-cadherin levels were variable but generally lower in tumour cells than in control astrocytes (Fig. 1C,E). Quantification showed a decrease of 91%±3.5 in the U138 cells and of 77%±7 in the U373 cells in the N-cadherin level compared with normal primary astrocytes (Fig. 1E). Diminution of N-cadherin protein levels was not associated with an increase in the expression of other classical cadherins, such as E-cadherin (supplementary material Fig. S1).

The decrease in N-cadherin expression was confirmed by immunofluorescence. In primary glioma cells (Fig. 1D) and glioma cell lines (Fig. 1F; supplementary material Fig. S2), N-cadherin staining appeared discontinuous, leaving empty spaces between adjacent cells. By contrast, in normal astrocytes, N-cadherin accumulated in regions of cell–cell contacts, forming a continuous line of adherens junctions between adjacent cells (Fig. 1F; supplementary material Fig. S2). Together, these results suggest that N-cadherin levels and adherens junctions are frequently downregulated in high-grade gliomas.

Decreased N-cadherin expression in primary astrocytes and glioma cells leads to a faster and less-directed migration

We next investigated whether differences in N-cadherin expression levels correlated with variations in the characteristics of cell migration. Wounding of a monolayer of primary rat astrocytes (see supplementary material Movie 1) induces a slow, cohesive and directed migration (Etienne-Manneville and Hall, 2001; Nobes and Hall, 1999). In the same assay, the trajectories of U373 and U138 glioma cells were longer, and less directed, than those of normal astrocytes, with cells often turning around or changing direction during migration (Fig. 1G). We also observed that, in contrast to normal astrocytes, glioma cells often escaped the monolayer and migrated as individual cells. U138 cells also showed a loss of contact inhibition and often migrated on top of one another without stopping or changing direction following contact (see supplementary material Movies 2, 3). As glioma cells divide more frequently than normal astrocytes and tend to form very dense monolayers, we tested whether the level of confluence was responsible for their high velocity and their non-persistent migration. Non-confluent U373 migrated faster and less persistently than in confluent culture conditions (Fig. 2A,B), suggesting that confluence acts as a brake rather than a driving force for glioma cell migration.

The extensive genetic alterations that characterize gliomas limit their direct comparison with normal astrocytes (McLendon et al., 2008). To overcome this problem and determine the specific contribution of N-cadherin in cell migration, we used a siRNA approach to reduce N-cadherin levels in glioma cells and primary astrocytes. Downregulation of N-cadherin in U373 cells led to a faster and less-persistent migration, similar to that of U138 (Fig. 2A–C). In primary astrocytes, two different sequences induced, respectively, a 93%±5.5 and a 94%±4 reduction of N-cadherin protein levels (Fig. 2D). Downregulation of N-cadherin in primary astrocytes increased cell velocity and decreased migration persistence, reminiscent of that of glioma cells (Fig. 2A,B). Adherens junctions were severely reduced but not totally absent from N-cadherin-depleted astrocytes. Cell–cell contacts were less stable, and, upon wounding, the front rows of N-cadherin-depleted cells often detached from the monolayer and migrated as isolated cells (supplementary material Movie 4). However, N-cadherin-depleted astrocytes did not migrate as fast as glioma cells and still exhibited contact inhibition, suggesting that loss of N-cadherin strongly perturbs cell migration but also that additional alterations of the tumour cells contribute to their abnormal migration.

We conclude that N-cadherin participates in the regulation of the speed and direction of glial cell migration and that low N-cadherin levels in glioma cells promote a faster and less-directed migration and might ultimately strongly influence the invasive behaviour of glioblastomas. This correlation between a low N-cadherin level and faster and less-persistent migration led us to investigate whether and how N-cadherin levels might affect cell migration.

N-cadherin is required for astrocyte polarization during migration

To better characterize the migration defects observed in cells expressing low levels of N-cadherin, we analyzed the intracellular organization of the cytoskeleton. Directed astrocyte migration is associated with the formation of an elongated protrusion in the direction of migration that corresponds to the polarized reorganization of the actin and microtubule cytoskeletons (Etienne-Manneville and Hall, 2001; Osmani et al., 2006). By contrast, U373 and U138 cells formed short and unstable protrusions. In glioma cell lines, the actin and microtubule networks did not show a polarized organization (Fig. 3A). Similar alterations were observed in N-cadherin-depleted astrocytes (Fig. 3A). Thus, we further analyzed the

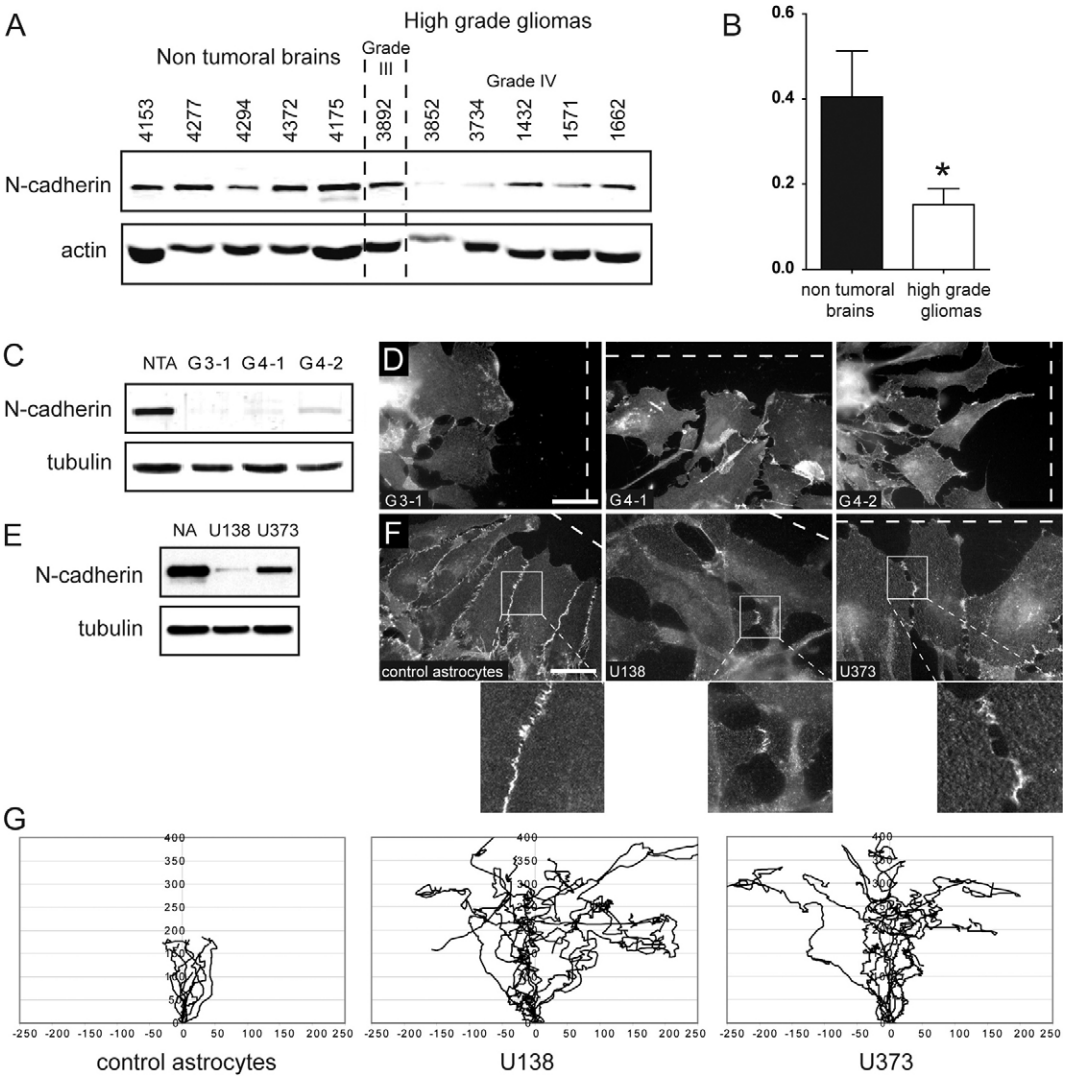

Fig. 1. Downregulation of N-cadherin protein levels in glioma cell lines correlates with nondirected migration. (**A**) Anti-N-cadherin and anti-β-actin western blot analysis of total protein extracts from primary high-grade gliomas and control brain samples. (**B**) Quantification of fluorescence intensity after N-cadherin western blotting indicates a threefold decrease of N-cadherin protein levels in glioblastomas compared with normal brain (Student's *t*-test, $*P<0.05$). (**C**) Anti-N-cadherin and anti-β-tubulin western blot analysis of total protein extracts from non-tumoural astrocytes (NTAs) and three cell lines (G3-1, G4-1 and G4-2) established from human fresh tissue samples. N-cadherin protein levels are strongly decreased in the three cell lines in comparison with non-tumoural astrocytes. (**D**) Immunofluorescence images showing N-cadherin localization in fresh tissue- sample-derived cells revealing that they form almost no contacts with one another. The broken lines show the position of the wound. (**E**) Anti-N-cadherin and anti-β-tubulin western blot analysis of total protein extracts from primary astrocytes (NA), U138 and U373 cell lines. U138 cells show only faint N-cadherin protein levels, whereas diminution in U373 cells is less important. (**F**) Immunofluorescence images showing N-cadherin localization in migrating control astrocytes, U138 and U373 cells. The two cell lines exhibit only small areas with intercellular contacts. Thick broken lines show the position of the wound. The lower panels show a high magnification of the boxed areas in the images above. Image contrasts have been adjusted to render N-cadherin staining visible in all cell types. Non-modified images can be seen in supplementary material Fig. S2. (**G**) Diagrams representing the migration trajectories covered in 36 hours of ten representative cells in primary rat astrocytes (supplementary material Movie 1), U138 and U373 glioma cell lines (supplementary material Movies 2 and 3). Scale bars: 35 μm for control astrocytes, G3-1, G4-1 and G4-2 and 25 μm for U373 and U138 cells.

impact of N-cadherin levels on glial cell polarization. The relative position of the centrosome, which is also the microtubule-organizing centre (MTOC), and the nucleus is a good indicator of cell polarity. In migrating astrocytes, the centrosome and the Golgi apparatus localize in front of the nucleus in the direction of migration (Etienne-Manneville and Hall, 2001; Etienne-Manneville et al., 2005). Reorientation of the centrosome and the Golgi apparatus was strongly perturbed in both glioma cell lines (Fig. 3B). However, U373 cells, which express a higher level of N-cadherin than U138, were less affected than U138 (41% vs 30%; $P<0.05$) (Fig. 3C). We then tested whether changes in N-cadherin expression levels could affect glioma cell polarity. Increased downregulation of the level of N-cadherin in U373 cells by siRNA further altered centrosome reorientation in these cells, whereas control siRNA had no effect (Fig. 3C). Interestingly, only 31% of N-cadherin-depleted U373 cells had a correctly oriented centrosome. This percentage was similar to that of U138 cells and not statistically different from

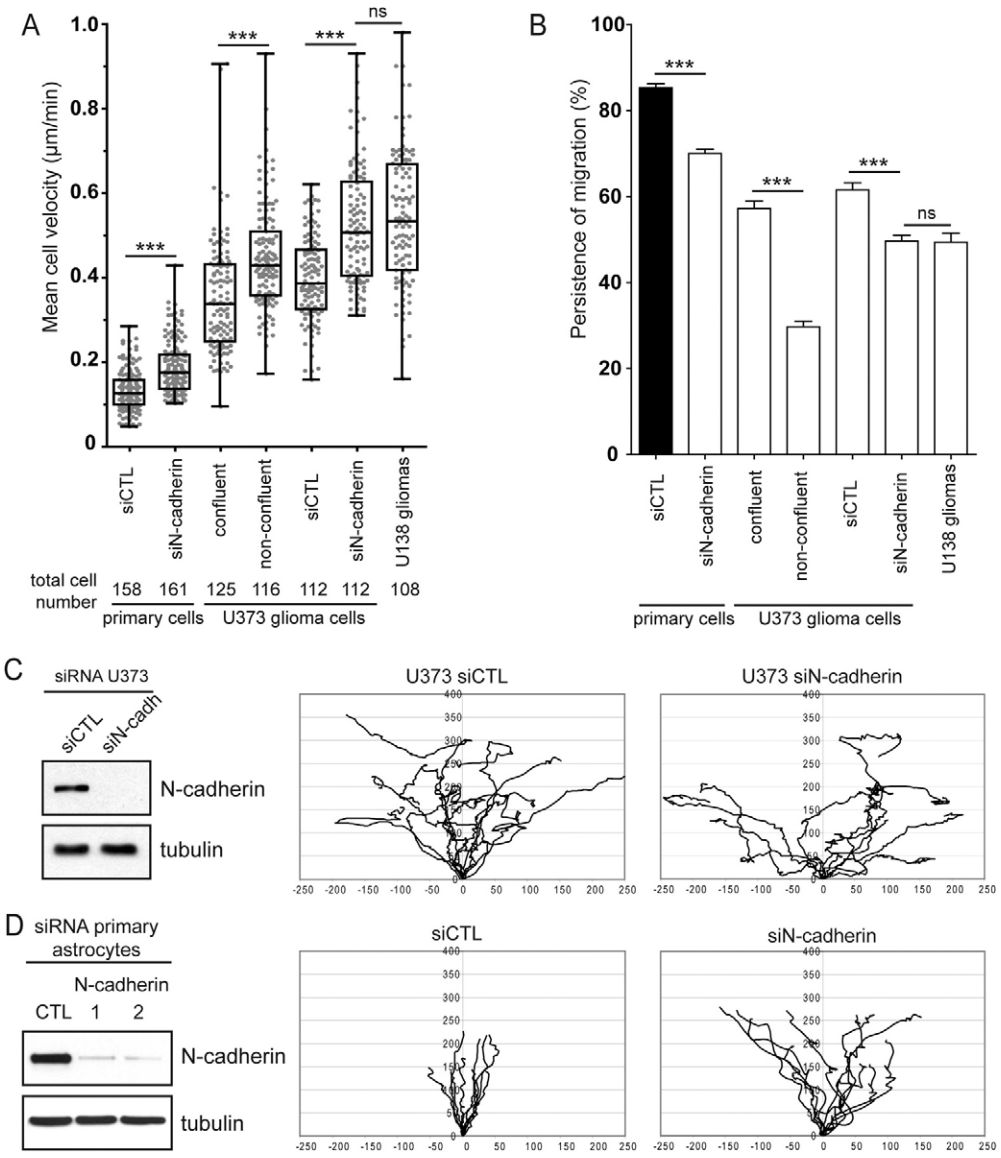

Fig. 2. Loss of N-cadherin in primary astrocytes and glioma cells leads to a faster and less-directed migration. (**A**) Box-and-whisker plots overlaid with the mean velocity obtained for each tracked cell. The boxes represent the 25th and 75th percentile of the data, and the line bisecting the box corresponds to the median (***$P<0.001$; ns, nonsignificant). N-cadherin depletion in primary astrocytes, as well as in U373 glioma cells, leads to an increase in cell velocity. U138 glioma cells, showing the lower levels of N-cadherin, are the faster ones. Non-confluent culture conditions for U373 cells also increases their average velocity. (**B**) Histogram showing the persistence of migration expressed as a percentage. It represents the ratio between the vectorial distance and the mean distance (see Materials and Methods) (***$P<0.001$). N-cadherin depletion in primary astrocytes, as well as in U373 glioma cells, induces a less-persistent migration of the cells in one given direction. The least-persistent migration is observed in non-confluent culture conditions. (**C**) Anti-N-cadherin and anti-β-tubulin western blot analysis of total protein extracts from U373 cells after control (CTL) or N-cadherin-specific siRNA nucleofection (siN-cadh). The diagrams represent the migration trajectories covered in 36 hours of ten representative cells in U373 cells nucleofected with control or N-cadherin siRNA. (**D**) Anti-N-cadherin and anti-β-tubulin western blot analysis of total protein extracts from primary astrocytes after control (CTL) or N-cadherin-specific siRNA nucleofection. The diagrams represent the migration trajectories covered in 36 hours of ten representative cells in primary astrocytes nucleofected with control or N-cadherin siRNA (supplementary material Movie 4).

25%, which corresponds to a totally random centrosome orientation. In normal astrocytes, depletion of N-cadherin and Ca^{2+} depletion, which prevents cadherin-mediated intercellular contacts, also profoundly altered centrosome reorientation (Fig. 3C). Taken together, these results show that the level of expression of N-cadherin is a crucial parameter in the control of polarity in normal astrocytes and in glioma cells.

N-cadherin-mediated contacts control the turnover of focal adhesions and spatially restrict their engagement to the leading edge

During wound healing, astrocyte polarization and directed migration are totally dependent on integrin engagement at the wound edge of the cells (Etienne-Manneville and Hall, 2001; Peng et al., 2008). Localized integrin signalling leads to the

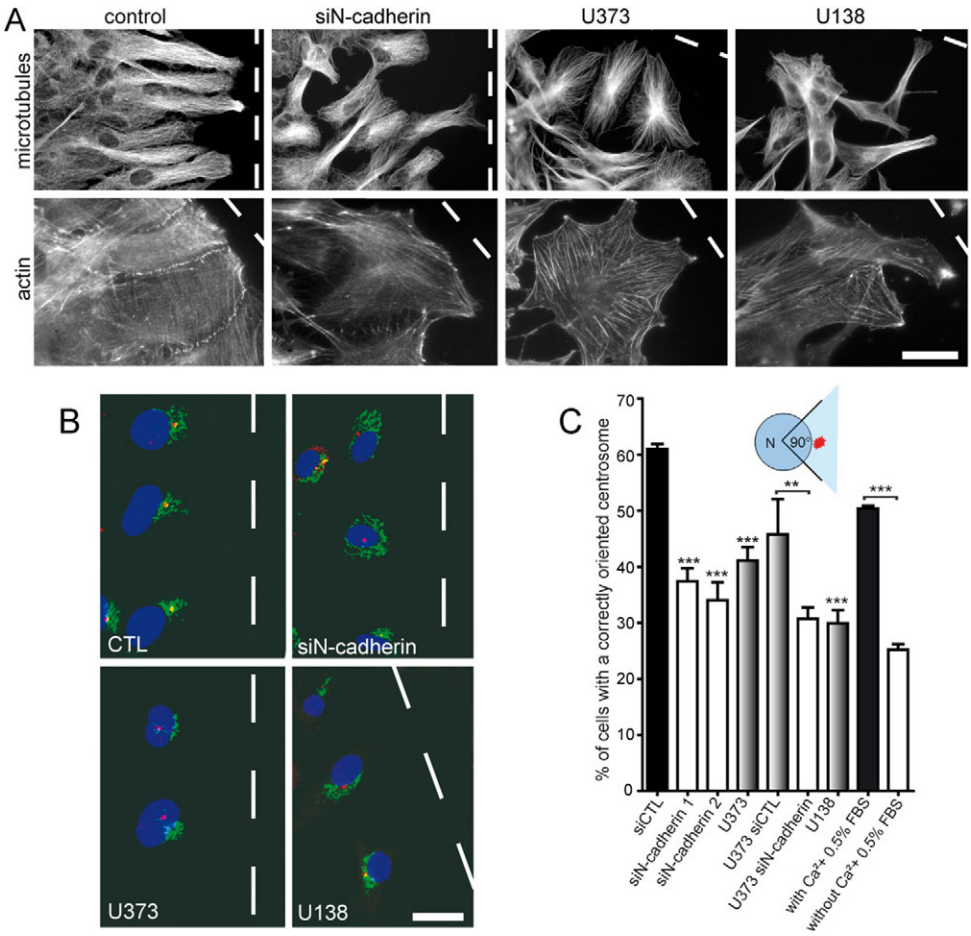

Fig. 3. N-cadherin is required for astrocyte polarization during migration. (**A**) Anti-α-tubulin and phalloidin stainings 8 hours after scratching showing the organization of microtubule and actin networks in control astrocytes (CTL), N-cadherin-depleted astrocytes (siN-cadherin), U373 and U138 glioma cells. (**B**) Immunofluorescence images showing anti-pericentrin (red, centrosome) and anti-GM130 (green, Golgi apparatus) immunostaining associated with Hoechst staining (blue, nucleus). (**C**) Histogram showing the percentage of cells with a correctly oriented centrosome 8 hours after wounding in each culture condition. Centrosomes located within the quadrant facing the wound, in front of the nucleus, were scored as correctly oriented (see Materials and Methods). For each time-point and each experimental condition, a minimum of 100 cells was scored. Results are shown as means ± s.e.m. of 3–5 independent experiments (***$P<0.001$; **$P<0.01$). Scale bars: 35 μm (upper panel) and 20 μm (lower panel) in A and 30 μm in B. The broken line shows the position of the wound.

polarized recruitment of the small GTPases Cdc42 and Rac (Osmani et al., 2010; Osmani et al., 2006), two major regulators of the microtubule and actin cytoskeletons and crucial modulators of the speed and direction of cell migration (Frame and Brunton, 2002; Watanabe et al., 2005).

In order to determine whether N-cadherin-reduced expression could influence cell–matrix adhesion, we first examined the distribution of focal adhesions in basal conditions without any scratch (Fig. 4A,B). Immunofluorescence staining for paxillin, a major component of the integrin-mediated signalling pathway, showed that non-confluent glioma cells had a significantly higher number of focal adhesions than normal astrocytes (Fig. 4A,C) and that the mean size of these focal adhesions was smaller (Fig. 4D). Depletion of N-cadherin in astrocytes was sufficient to induce a strong increase in focal adhesion number, as well as a decrease in focal adhesion size (Fig. 4A,C,D). These effects were not due to a difference in cell size (Fig. 4E). These observations suggest that N-cadherin levels influence the formation of focal adhesions in non-confluent cells.

When confluent, control astrocytes were strongly adhesive with one another, and few focal adhesions were detectable using paxillin staining (Fig. 4B). By contrast, numerous focal adhesions were visible in glioma cells as well as in confluent N-cadherin-depleted astrocytes (Fig. 4B), suggesting that N-cadherin-mediated contacts prevent formation of focal adhesions.

In control primary astrocytes, scratching induced a major increase in the number of focal adhesions at the wounded edge (Fig. 4F). Just after wounding, paxillin was essentially cytoplasmic, with very few detectable focal contacts. One hour after wounding, paxillin localized in focal adhesions that accumulated at the front edge of the cells and were polarized in the direction of the wound (Fig. 4G). As reported previously (Borghi et al., 2010; Dupin et al., 2009), paxillin and N-cadherin stainings in normal astrocytes showed a mutual exclusion between focal adhesions and adherens junctions (Fig. 5A), confirming the inhibitory role of cadherin-mediated contacts on formation of focal adhesions. By contrast, focal adhesions were present at the entire periphery of glioma cells prior to wounding, and the distribution of focal adhesions was not modified in response to the wound and showed no preferential localization regarding the wound orientation (Fig. 4G). N-cadherin depletion in astrocytes strongly affected wound-induced formation of focal adhesions at the wound edge. As in glioma cells, the number and localization of focal adhesions did not significantly change following wounding (Fig. 4F,G). Focal adhesions were found at the front as well as the back of the cells and were not excluded from regions of cell–cell contacts (Fig. 5A). We conclude that reduction of N-cadherin levels and inhibition of N-cadherin-mediated contacts strongly affects the distribution of focal adhesions and prevents wound-induced formation of focal adhesions at the wound edge of the cells.

N-cadherin is involved in the decrease of Src inhibitory phosphorylation on Y529 in response to the wound

Downstream of integrins, activation of Src-like kinases is required for polarized migration of astrocytes (Etienne-Manneville and

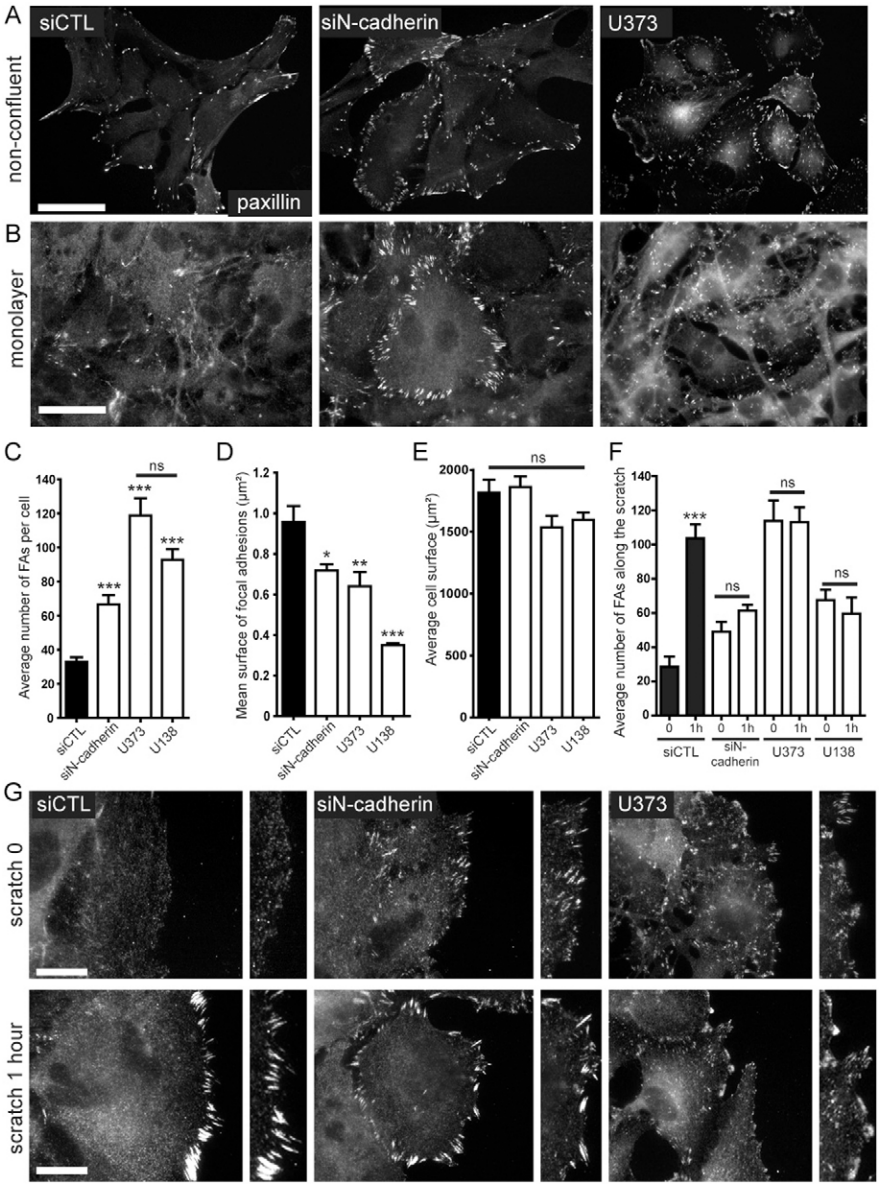

Fig. 4. N-cadherin is involved in the control of the formation of focal adhesions and of their spatial restriction in response to the wound. (**A**,**B**) Paxillin immunostaining in control astrocytes (siCTL), N-cadherin-depleted astrocytes (siN-cadherin) and U373 glioma cells. Cells were fixed without scratching under non-confluent conditions (A) or confluent conditions (B; monolayer). (**C**) Histogram showing the average number of focal adhesions (FAs) in each indicated cell type based on paxillin immunostaining under non-confluent conditions (***$P<0.001$; ns, nonsignificant). (**D**) Histogram showing, for each indicated cell type, the mean surface occupied by focal adhesions based on paxillin immunostaining under non-confluent conditions for each cell type (***$P<0.001$; **$P<0.01$; *$P<0.05$). (**E**) Histogram showing, in each indicated cell type, the average surface occupied by individual cells under non-confluent conditions (ns, nonsignificant). (**F**) Histogram showing the average number of focal adhesions (FAs) at the leading edge of wounded cells, just after (time 0) or one hour after the scratch (time 1h), in each indicated cell type (***$P<0.001$; ns, nonsignificant). (**G**) Paxillin immunostaining in control astrocytes (siCTL), N-cadherin-depleted astrocytes (siN-cadherin) and U373 glioma cells. Cells were fixed and stained just after (scratch 0) or one hour (scratch 1h) after scratching. The small panels on the right of each image show a high magnification of the front edge of the cells. Scale bars, 20 µm in A and G and 35 µm in B. The broken line shows the position of the wound.

Hall, 2001). In particular, the activity of Src, a tyrosine kinase activated following integrin engagement (Guarino, 2010), is tightly regulated by its phosphorylation state on two principal tyrosine residues, the activating Y418 and the inhibiting Y529. Both phosphorylations have been shown to be involved in the turnover of focal adhesions and tumour invasion (Guarino, 2010).

Although we could not detect a significant increase in Y418 phosphorylation, Src Y529 phosphorylation was strongly decreased during the first hour following wounding of control astrocytes (Fig. 5B). Double phospho-Src Y529 and paxillin staining showed that the dephosphorylation of Src Y529 was concentrated at the leading front of migrating astrocytes (Fig. 5C) and suggested that decreased phosphorylation was associated with focal adhesion formation and signalling. In N-cadherin-depleted astrocytes and in glioma cells, Src Y529 phosphorylation did not decrease following wounding and even increased during this time (Fig. 5B). Moreover, phosphorylated Src Y529 was found in most focal adhesions, irrespective of the wound orientation (Fig. 5C). These results indicate that N-cadherin-mediated contacts are required to restrict integrin-mediated signalling in time and space.

N-cadherin-mediated contacts are required for integrin-mediated recruitment of βPIX at the leading edge

Upon wounding, the Rho guanine nucleotide exchange factor 7 (hereafter referred to as βPIX) is recruited to the wound edge of astrocytes, where it induces Cdc42 and Rac recruitment and activates Cdc42 to promote cell polarization and migration (Osmani et al., 2006). βPIX is known to interact with focal adhesion proteins (Frank and Hansen, 2008) and to be activated by Src (Feng et al., 2010).

Cell treatment with a cyclic RGD peptide to block integrin engagement with the extracellular matrix and the phosphatase PP2, a specific inhibitor of Src-like protein kinases, significantly decreased βPIX recruitment to the leading edge (Fig. 6A),

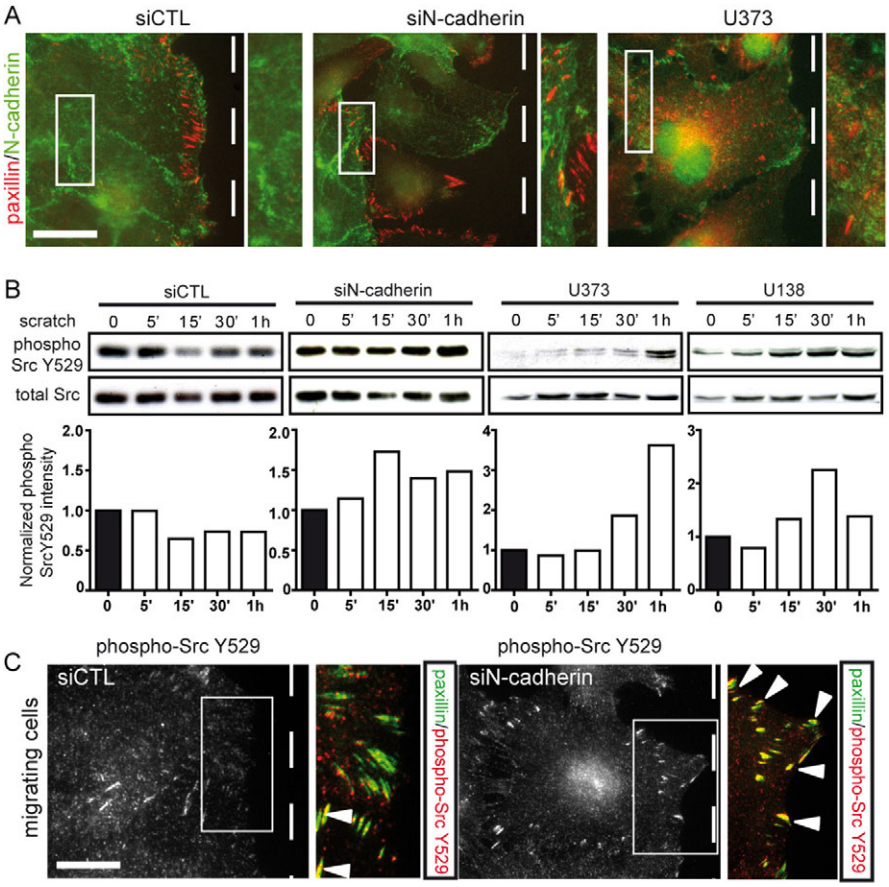

Fig. 5. N-cadherin is involved in the diminution of Src-inhibitory phosphorylation on tyrosine 529 in response to the wound. (**A**) Paxillin and N-cadherin double immunostaining one hour after scratching in control astrocytes (siCTL), N-cadherin-depleted astrocytes (siN-cadherin) and U373 glioma cells. The broken lines show the position of the wound. The small panels show a high magnification of the rear of the cells (bottom panel). The contrast of the images has been modified so as to compare the different culture conditions. See supplementary material Fig. S2 for unmodified contrast. (**B**) Anti-phospho-Src Y529 and anti-Src western blot analysis of total protein extracts from control astrocytes (siCTL), N-cadherin-depleted astrocytes (siN-cadherin), U373 and U138 glioma cells at the indicated time after scratching. The quantification is shown beneath each corresponding blot. (**C**) Specific phospho-Src Y529 immunostaining in control astrocytes (siCTL) and N-cadherin-depleted astrocytes (siN-cadherin) while migrating 8 hours after the scratch. The broken lines show the position of the wound. The two small panels show a high magnification of paxillin (green) and phospho-Src Y529 (red) immunostaining at the leading edge. Scale bars: 20 μm in A and 15 μm in C.

showing that wound-induced integrin signalling is required for leading edge recruitment of βPIX in migrating astrocytes. As N-cadherin depletion impaired wound-induced integrin engagement, we asked whether it consequently affected integrin-mediated βPIX recruitment at the cell leading edge. The percentage of cells exhibiting βPIX immunofluorescence at the wound edge was significantly reduced in N-cadherin-depleted astrocytes compared with control cells (Fig. 6A–C). Similarly, the localization of βPIX at the leading edge of U138 and U373 cells was barely detectable (Fig. 6B,C).

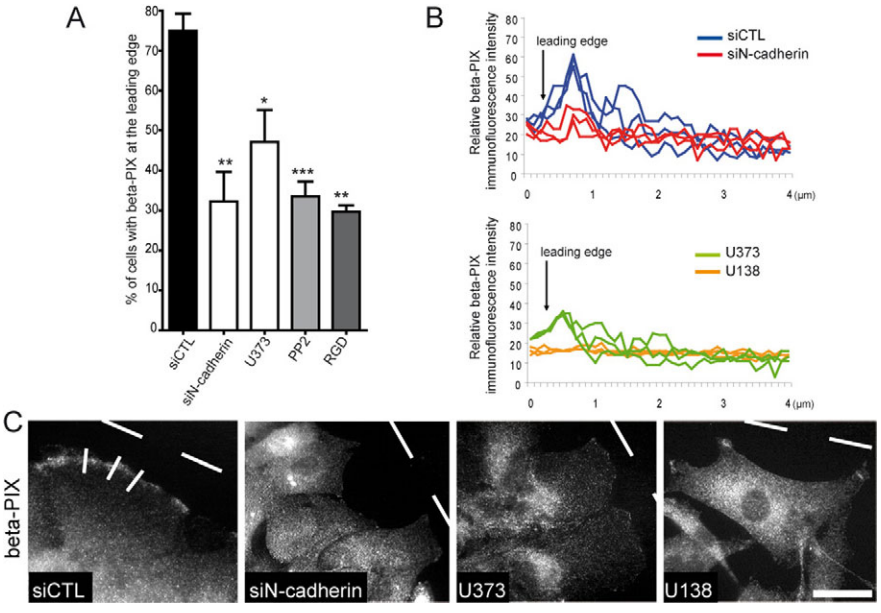

Fig. 6. N-cadherin-mediated contacts are required for integrin-mediated recruitment of βPIX at the leading edge. (**A**) Histogram showing the percentage of cells with βPIX immunofluorescence at the leading edge in the different culture conditions. PP2 is an inhibitor of Src-like tyrosine kinases, and cyclic RGD peptide specifically inhibits integrin engagement with the extracellular matrix (***$P<0.001$; **$P<0.01$; *$P<0.05$). (**B**) Graphs showing, for each indicated cell type, three representative profiles corresponding to βPIX fluorescence intensity along three different lines across the cell edges. (**C**) βPIX immunostaining 4 hours after scratching in control astrocytes (siCTL), N-cadherin-depleted astrocytes (siN-cadherin), U373 and U138 glioma cells. Scale bar: 30 μm. The broken line shows the position of the wound.

Wound-induced Cdc42 polarized activation and Cdc42-dependent polarity pathway are altered in N-cadherin-depleted astrocytes and glioma cell lines

The role of N-cadherin in the regulation of focal adhesions and βPIX recruitment to the wounded cell front prompted us to test whether N-cadherin levels could modulate the regulation of the βPIX target Cdc42 (Feng et al., 2004; Osmani et al., 2006). Cdc42 is an evolutionarily conserved regulator of cell polarity (Etienne-Manneville, 2004) and plays a key role in astrocyte polarization and directed migration (Etienne-Manneville and Hall, 2001; Osmani et al., 2006). During wound healing, βPIX activates and recruits Cdc42 at the leading edge (Cau and Hall, 2005; Etienne-Manneville and Hall, 2001; Osmani et al., 2006; Shen et al., 2008).

Astrocytes of the migrating front were microinjected with a GFP-tagged wild-type Cdc42 construct. Upon wounding, GFP–Cdc42 was recruited to the cell leading edge of control astrocytes (Fig. 7A,B), as previously described (Etienne-Manneville and Hall, 2001; Osmani et al., 2006). GFP–Cdc42 was cytosolic and also associated with the Golgi apparatus and perinuclear membranes (Etienne-Manneville and Hall, 2001; Michaelson et al., 2001; Osmani et al., 2006). In migrating U138 and U373 cells, GFP–Cdc42 was still present on intracellular membranes but was not enriched at the leading edge of the cells (Fig. 7A,B). Similarly, N-cadherin depletion in primary astrocytes did not affect Cdc42 localization on perinuclear membranes but prevented GFP–Cdc42 recruitment to the cell leading edge (Fig. 7A,B). This inhibition of Cdc42 recruitment was not due to the alteration of membrane protrusion as we have previously shown that the recruitment of Cdc42 at the leading edge was independent of cell protrusion (Osmani et al., 2010).

We then used a pulldown assay to assess Cdc42 activation following wounding. Scratch-induced activation of Cdc42 was dramatically reduced in U138 and U373 cells as well as in N-cadherin-depleted astrocytes (Fig. 7C). Despite the different expression level of N-cadherin between U373 and U138, we could not detect any difference between these cells in the regulation of Cdc42 localization and activity in response to wounding. The low N-cadherin levels observed in U373 might not be sufficient to generate a wound-induced signal. It is also possible that our detection methods are not sensitive enough to detect a limited Cdc42 activation. However, these results show that N-cadherin is required for integrin- and βPIX-mediated activation and recruitment of Cdc42 at the leading edge of migrating astrocytes.

During wound-induced migration, active Cdc42 binds to the Par6–PKCζ complex to promote PKCζ activation (Etienne-Manneville and Hall, 2001). In turn, the Par6–PKCζ complex controls centrosome reorientation by inducing adenomatous polyposis coli (APC) clustering at the plus-end of leading edge microtubules (Etienne-Manneville and Hall, 2003). Par6 and PKCζ showed a cytoplasmic distribution, with a specific enrichment at the leading edge of control migrating astrocytes (Fig. 8A,B). Par6 was also localized to the nucleus (Fig. 8A), and PKCζ was also associated with some intercellular contacts (data not shown), as already described for other cell types (Izumi et al., 1998; Manabe et al., 2002). In N-cadherin-depleted astrocytes, U373 and U138 cells, the leading edge recruitment of both Par6 and PKCζ was strongly perturbed (Fig. 8A,B), and the percentage of cells exhibiting Par6 or PKCζ immunofluorescence at the leading edge was significantly decreased (Fig. 8C). APC recruitment to leading edge microtubules was strongly reduced in

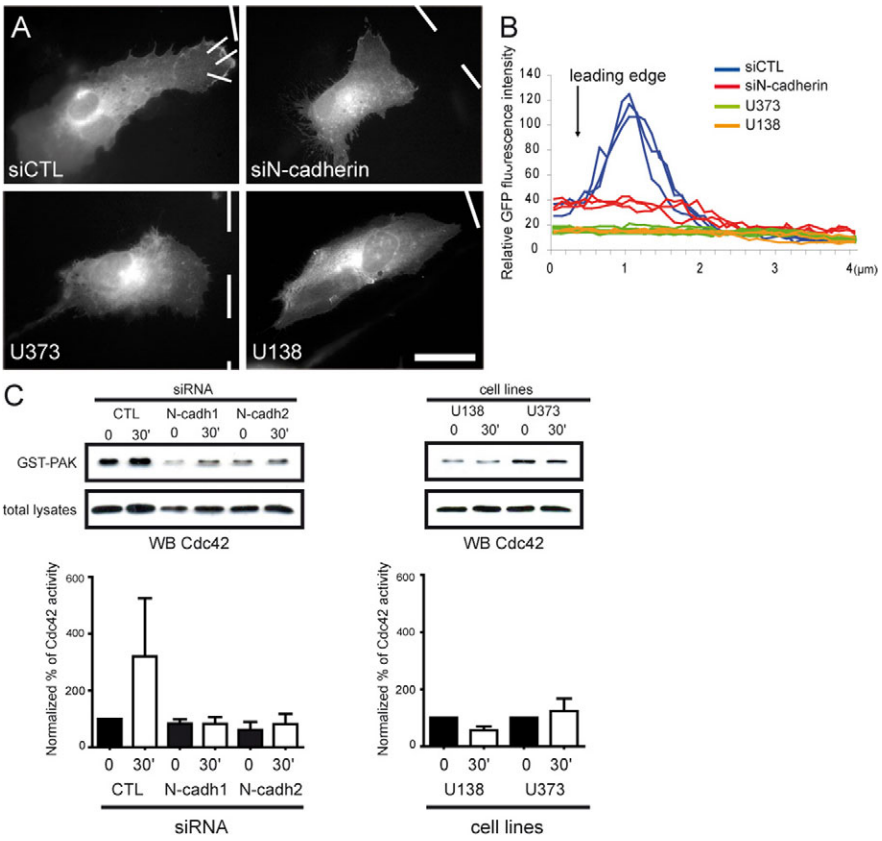

Fig. 7. Scratch-induced recruitment and activation of Cdc42 at the leading edge is lost in N-cadherin-depleted astrocytes and glioma cells.
(**A**) Microinjection of a GFP-tagged Cdc42 construct reveals the localization of Cdc42 in the different cell types. (**B**) Three representative intensity profiles corresponding to GFP–Cdc42 fluorescence intensity along three different lines drawn across the cell front edge (as shown in the siCTL panel of A). (**C**) Western blots showing active Cdc42 (as determined by GST–PAK pulldown assay) and total Cdc42, 0 or 30 minutes after scratching in control and N-cadherin-depleted astrocytes (left panel) and in glioma cell lines (right panel). Histograms represent the normalized Cdc42 activity 0 and 30 minutes after scratching. Results are shown as means ± s.e.m. of 3–7 independent experiments. Scale bar: 30 μm in A. The broken line shows the position of the wound.

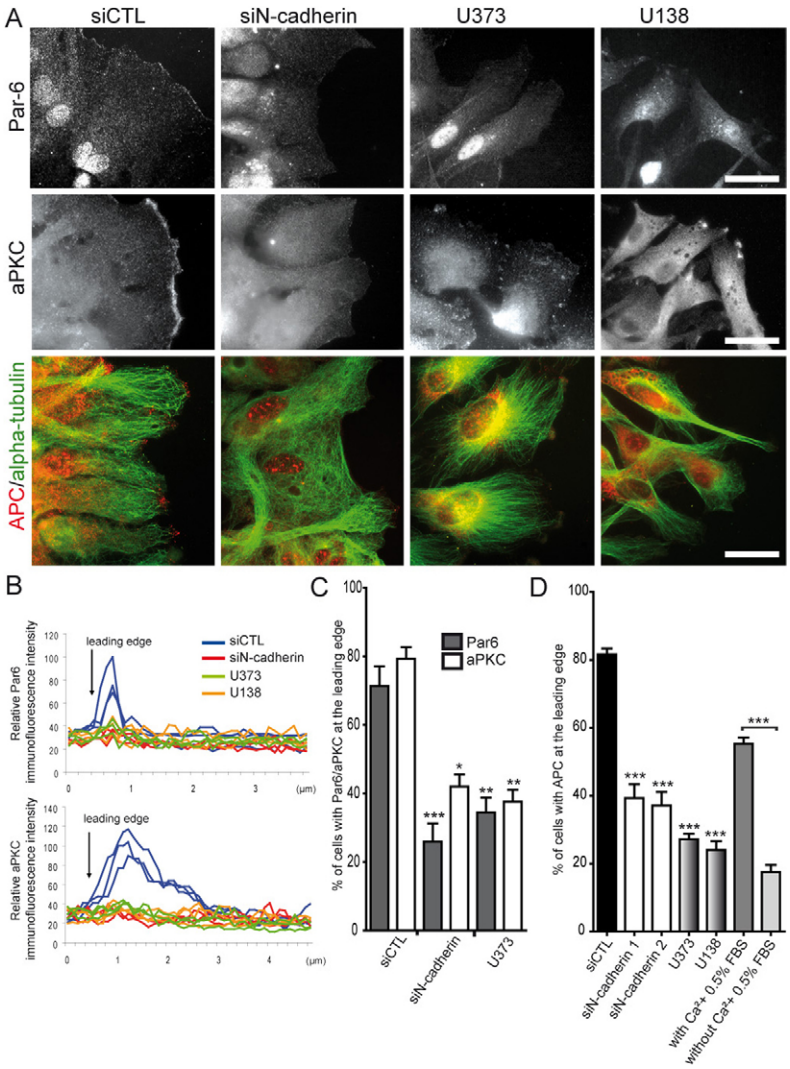

Fig. 8. The Cdc42-dependent polarity pathway is altered in gliomas and N-cadherin-depleted astrocytes. (**A**) Fluorescence images showing Par6, PKCζ, as well as APC (red) and α-tubulin (green) immunostaining in control astrocytes (siCTL), N-cadherin-depleted astrocytes and glioma cell lines. (**B**) Graphs showing, for each indicated cell type, three representative profiles corresponding to Par6 (higher panel) and PKCζ (lower panel) fluorescence intensity along three different lines across the cell edges. (**C**) Histogram showing the percentage of migrating cells with an accumulation of Par6 (dark grey) or PKCζ (white) at the leading edge (***$P<0.001$; **$P<0.01$; *$P<0.05$). (**D**) Histogram showing the percentage of cells in which APC formed clusters at the plus-ends of leading edge microtubules. This recruitment is lower after N-cadherin depletion or in low-Ca^{2+} culture medium, as well as in U373 cells, than in the control astrocytes. For each time-point and each experimental condition, a minimum of 100 cells were scored. Results are shown as means ± s.e.m. of three independent experiments (***$P<0.001$). Scale bars: 25 μm. The broken line shows the position of the wound.

U373 and U138 as well as after N-cadherin depletion in astrocytes (Fig. 8A,D). This effect was also observed in astrocytes cultured in a Ca^{2+}-depleted medium (Fig. 8D). Our results show that N-cadherin-mediated intercellular contacts control the integrin-dependent polarity pathway that regulates centrosome positioning and directed astrocyte migration.

Rescuing N-cadherin expression restores cell polarity and inhibits glial cell migration

As N-cadherin expression appears necessary for wound-induced astrocyte polarization, we investigated whether the absence of N-cadherin was responsible for the altered polarity of glioma cells. We expressed a siRNA-resistant GFP-tagged N-cadherin construct in N-cadherin-depleted cells and glioma cell lines (Fig. 9A). Nucleofection of the GFP vector with control or N-cadherin siRNA had no effect on centrosome reorientation (Fig. 9A,B). By contrast, expression of GFP–N-cadherin in N-cadherin-depleted astrocytes rescued centrosome reorientation, further demonstrating the role of N-cadherin in cell polarity (Fig. 9B). Interestingly, expression of N-cadherin also had a dramatic effect on the polarization of U373 and U138 cells. In both cell lines, wound-induced centrosome reorientation was restored and the percentage of polarized cells was almost the same as that of normal astrocytes (Fig. 9A,B). These results indicate that a decrease of N-cadherin expression is a major event perturbing polarity during glioma cell migration.

Finally, we wanted to determine whether loss of N-cadherin was responsible for the abnormal migration of glioma cells. We performed live experiments on GFP-tagged N-cadherin-expressing glioma cell lines. Expression of the GFP vector led to slight changes in the average velocity of both glioma cell lines (0.410 ± 0.010 μm $minute^{-1}$ for U373 GFP and 0.456 ± 0.016 μm $minute^{-1}$ for U138 GFP) (Fig. 9C). These changes might be due to GFP expression, nucleofection itself and/or the selection of a more restricted population of cells in these experiments. We thus compared the migratory behaviour of GFP-expressing glioma cells with that of N-cadherin GFP-expressing glioma cells. We observed that long-term expression of N-cadherin in glioma cells was frequently toxic. We did not investigate the reasons for this toxicity, which seems specific to N-cadherin (data not shown), and suffering cells were excluded from our analysis. We observed that N-cadherin-expressing glioma cells migrated in a limited space area in comparison with their control counterparts (Fig. 9C,D). Interestingly, increased N-cadherin expression in glioma cell lines strongly reduced their mean velocity (0.318 ± 0.015 μm $minute^{-1}$ for rescue U373 and 0.236 ± 0.023

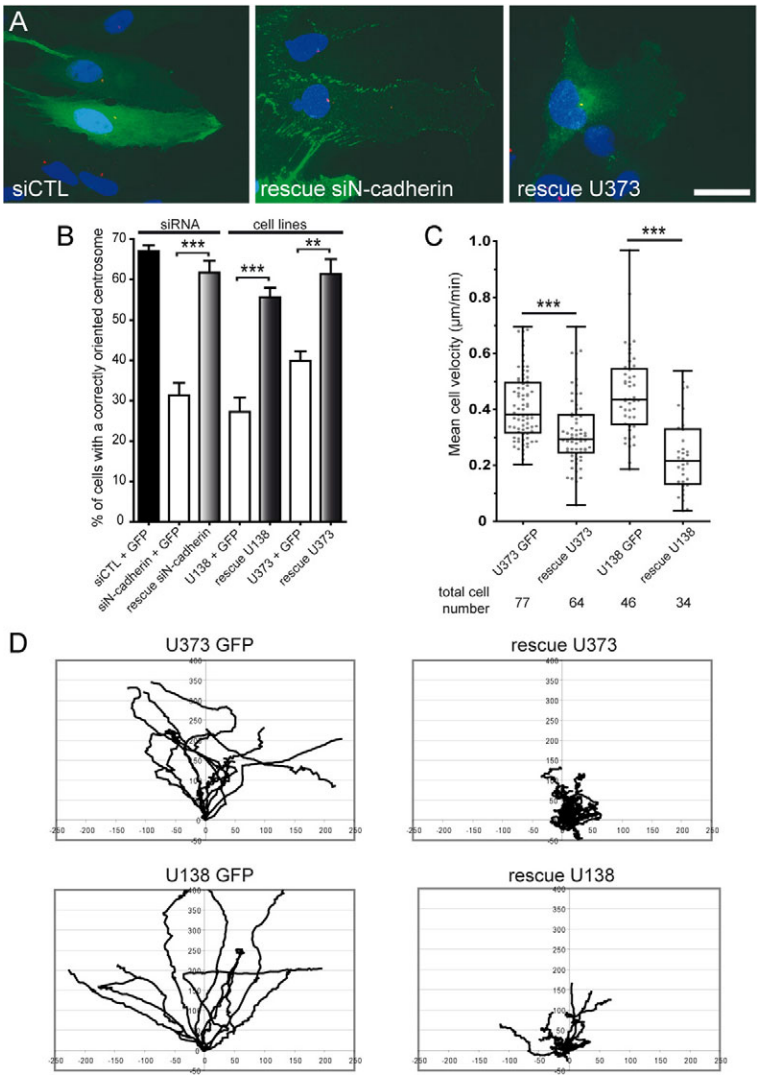

Fig. 9. Exogenous expression of N-cadherin rescues centrosome orientation and reduced glioma cell velocity. A wound-induced migration assay was performed using control astrocytes (siCTL), N-cadherin-depleted astrocytes (siN-cadherin), U373 and U138 glioma cells nucleofected, or not nucleofected, with the pEGFP–N-cadherin construct. (**A**) Fluorescence image showing GFP expression (green, pEGFP–N-cadherin), pericentrin immunostaining (red, centrosome) and Hoechst staining (blue, nucleus). (**B**) Histogram showing the percentage of cells with a correctly oriented centrosome 8 hours after wounding for each culture condition. Results are shown as means ± s.e.m. of 3–5 independent experiments (***$P<0.001$; **$P<0.01$). (**C**) Box-and-whisker plots overlaid with the mean velocity obtained for each tracked cell. The boxes represent the 25th and 75th percentile of the data, and the line bisecting the box corresponds to the median (***$P<0.001$). (**D**) Diagrams representing the migration trajectories of ten representative cells in primary rat astrocytes and glioma cell lines. Scale bar: 30 µm in A. The broken line shows the position of the wound.

µm minute^{-1} for rescue U138) (Fig. 9C). However, it did not restore the directed and coordinated migration, possibly because the proportion of N-cadherin-expressing cells was not sufficient. These results confirm that N-cadherin acts as a brake to cell migration and that the decreased expression of N-cadherin participates, with other molecular changes, in the abnormal migration of glioma cells.

Discussion

Role of intercellular adhesion molecules in the migration behaviour of glioma cells

Intercellular adhesion together with adhesion to the extracellular matrix play a crucial role in the establishment and maintenance of cell polarity in developing and mature tissues. In tumour cells, loss of polarity is now considered as one of the triggering signals of tumourigenesis and invasion of the surrounding tissue (Humbert et al., 2003; Iden and Collard, 2008). In the case of epithelial cancers, polarity alteration occurs through an epithelial–mesenchymal transition (EMT) that is believed to be one of the major processes involved in tumour progression and metastasis (Kang and Massague, 2004; Micalizzi et al., 2010; Thiery, 2002). An EMT results from several molecular changes, consisting of a global loss of epithelial markers, including E-cadherin, and an accompanying gain of mesenchymal markers such as N-cadherin (Kuphal and Bosserhoff, 2006; Maeda et al., 2005; Nakajima et al., 2004). In this situation, N-cadherin has a promigratory effect, helping the tumour cells to detach from their normal location and to spread in their environment (Agiostratidou et al., 2007; Hazan et al., 2004).

In the central nervous system, cells do not express E-cadherin but mainly N-cadherin, and no switch between cadherins has been described in the case of malignant gliomas, except in some specific cases (Lewis-Tuffin et al., 2010). Changes in N-cadherin expression are still controversial mainly owing to the observation of an inverse correlation between N-cadherin mRNA and protein levels (Asano et al., 2004; Shinoura et al., 1995), which we also observed (data not shown). This discrepancy most probably reflects defects in protein synthesis or stability. Catenins might be involved in this phenomenon as they have been shown to stabilize cadherin interactions (Reynolds and Carnahan, 2004; Xiao et al., 2007). In favour of this hypothesis, we observed a low expression level of catenins in glioma cell lines, as well as in fresh tissue-sample-derived cells (data not shown).

When only considering N-cadherin protein expression, it has been shown to be either downregulated (Asano et al., 1997; Asano et al., 2000; Foty and Steinberg, 2004; Hegedus et al., 2006) or upregulated (Utsuki et al., 2002), and its precise role in glial cell migration is still unknown. Our observations made in glioma samples, in tissue-sample-derived glioma cells and in glioma cell lines suggest that N-cadherin expression is variable but generally diminished in high-grade gliomas compared with normal primary glial cell cultures. Using a siRNA approach as well as rescue experiments, we show that N-cadherin is involved in the control of astrocyte and glioma cell velocity, which is in agreement with previous studies performed in other cell lines. Overexpression of N-cadherin in the C6 glioma cell line indeed leads to a significant decrease in their invasive behaviour (Asano et al., 2004), whereas a decrease of N-cadherin in LN18 cells induces an increase in cell migration (Rappl et al., 2008). Following siRNA-induced depletion of N-cadherin, astrocyte velocity is also increased. However, a decrease in N-cadherin levels cannot be solely responsible for the abnormal velocity of glioma cells, which migrate much faster than N-cadherin-depleted astrocytes. It is tempting to speculate that some of the numerous genetic alterations observed in gliomas, such as the downregulation of the tumour suppressor PTEN, also contribute to this increased migration speed (Raftopoulou et al., 2004). Nevertheless, we observe that glioma cells migrate even faster when N-cadherin levels are further decreased and migrate slower when N-cadherin is re-expressed in these cells, confirming that changes in N-cadherin levels are likely to impact strongly on the migration speed of glioma cells. In theory, loss of N-cadherin without re-expression of other cadherins should mechanically favour tumour cell migration away from the initial tumour, by loosening cell–cell junctions. Accordingly, in vitro migration of N-cadherin-depleted astrocytes showed that cells tend to escape from the monolayer to migrate individually inside the wound – a behaviour rarely observed with N-cadherin-expressing normal astrocytes.

Other cell-adhesion molecules normally expressed in the central nervous system have been described as playing important roles in glioma cell migration. Expression of neural cell-adhesion molecule (NCAM) is, for instance, decreased in glioma cells (Andersson et al., 1991; Gratsa et al., 1997; Maidment et al., 1997), and an inverse correlation was found between the expression of one NCAM isoform and the WHO-defined grade of a human glioma cell (Duenisch et al., 2010). NCAM over-expression in tumour astrocytes leads to a significant decrease in their invasive behaviour (Edvardsen et al., 1994; Owens et al., 1998), whereas addition of polysialylated acid (PSA) on NCAM has been shown to facilitate glioma invasion (Suzuki et al., 2005). Finally, PSA-NCAM has been recently proposed as a biomarker for the prognosis of patients with glioblastomas (Amoureux et al., 2010).

Studies support the notion that alterations in the organization or processing of intercellular junction proteins are more important than the regulation of their expression for explaining the migratory behaviour of glioma cells (Kohutek et al., 2009; Perego et al., 2002; Shinoura et al., 1995). Thus, whatever the mechanism employed by tumour cells, the weakening of cell–cell adhesion in gliomas would facilitate their migration and invasion throughout the central nervous system.

Cadherin–integrin interplay in the control of glial cell migration and polarization

In a non-migration situation on micropatterned substrates, an anisotropic distribution between cadherin-mediated interactions and focal adhesions determines the cell polarity axis through nucleus and centrosome positioning (Desai et al., 2009; Dupin et al., 2009). We show here that, in migrating cells, loss of N-cadherin also dramatically perturbs cell polarity and directed migration. Wound-induced cell-directed migration is promoted by an integrin-dependent pathway involving Src-like tyrosine kinases and Rho GTPases (Etienne-Manneville and Hall, 2001). Following wounding, integrin-mediated signalling leads to the activation and the recruitment of the small G-proteins Cdc42 and Rac, which are essential regulators of cell polarization and orientation during migration (Hall, 2005). Modifications in expression and/or activation of these small G-proteins have been reported to contribute to cancer development (Vega and Ridley, 2008). We have previously shown that, following wounding, Cdc42 is activated and recruited to the leading edge of migrating astrocytes in a wound-healing assay and that localized activity of Cdc42 plays a key role in astrocyte polarization and directed migration (Etienne-Manneville and Hall, 2001; Osmani et al., 2010; Osmani et al., 2006). In agreement with a recent study realized in smooth muscle cells, by using a blocking antibody against N-cadherin (Sabatini et al., 2008), we show here that intercellular contacts are required for the recruitment and activation of Cdc42 at the leading edge in response to the wound. Active Cdc42 induces the recruitment and activation of the Par6–PKCζ polarity complex (Etienne-Manneville and Hall, 2001) and APC clustering at microtubule plus-ends (Etienne-Manneville and Hall, 2003). This polarity pathway is strongly altered in the N-cadherin-depleted astrocytes, as well as in glioma cell lines. As a consequence, centrosome reorientation does not occur. Exogenous expression of N-cadherin in N-cadherin-depleted cells and in glioma cells rescues centrosome reorientation, confirming the crucial role of N-cadherin in the control of cell polarity.

Interestingly, the migratory behaviour of N-cadherin-depleted astrocytes is strongly similar to that observed for β-null astrocytes (Peng et al., 2008), suggesting that these two kinds of adhesions act in the same pathway controlling cell migration (Gimond et al., 1999; Huttenlocher et al., 1998). While regulation of N-cadherin-mediated contacts by focal-adhesion-associated proteins such as focal adhesion kinase (FAK) or paxillin has been reported (Yano et al., 2004), less is known about the regulation of focal adhesion by N-cadherin. We show here that N-cadherin expression affects the localization, number and size of focal adhesions, as previously reported for E-cadherin (Borghi et al., 2010). The increased number and smaller size of focal adhesions observed in cells expressing a low level of N-cadherin suggest that N-cadherin controls focal adhesion turnover. These effects might involve the regulation of Src phosphorylation on Y529, which has been shown to influence the dynamics of focal adhesions (Pera et al., 2005; Vielreicher et al., 2007). Increased turnover of focal adhesions might thus be responsible for the effect of N-cadherin on cell migration (Gupton et al., 2007), promoting a faster mesenchymal-like migration in a wound-healing assay. In addition, the constitutive engagement of integrins at the cell periphery does not allow further stimulation upon wounding and therefore prevents the generation of wound-induced integrin-mediated signals. Finally, homogenous distribution of focal adhesions does

not allow the generation of a spatially localized signalling pathway and thus does not sustain a persistent directed migration. Thus, downregulation of N-cadherin in glioma cells might induce, as EMT in epithelial cancer cells, a decrease in intercellular contacts in favour of more-dynamic and less spatially regulated adhesions to the extracellular matrix, resulting in the abnormal migratory behaviour of these cells.

Conclusions

Adherens junction proteins are now considered as key players in tumour progression in different types of cancer. Creating N-cadherin-depleted astrocytes by using a siRNA approach constitutes a good model to investigate the involvement of N-cadherin in glioma cell migration. We show that the levels of N-cadherin strongly impact on glial cell polarity and promote a nondirected migration. In addition, the decrease in the levels of N-cadherin participates in the release of a migration brake caused by adhesive interactions with neighbouring cells and probably contributes to the increased cell velocity observed in glioma cells. Together, our results point to the downregulation of N-cadherin as an important event favouring the acquisition of the invasive properties of gliomas.

Materials and Methods

Cell cultures and scratch-induced migration

All procedures were performed in accordance with the guidelines approved by the French Ministry of Agriculture, following European standards. Glioblastoma samples were provided by the local Department of Neurosurgery from patients who had given written and informed consent, as approved by the local research ethics boards at the Salpêtrière Hospital. Samples were washed with Hanks balanced salt solution (Gibco, Invitrogen, Carlsbad, CA), dissected, sectioned and enzymatically dissociated with both 5 mg ml^{-1} of trypsin and 200 U ml^{-1} of DNAse (both from Sigma-Aldrich, St Louis, MO) for 10 minutes at 37℃. Erythrocytes were lysed using NH_4Cl. The cells were seeded into T75 flasks at 10,000 cells cm^{-2}. Cultures were incubated in 5% CO_2 at 37℃ in Dulbecco's modified Eagle's medium–F12 (Gibco, Invitrogen, Carlsbad, CA) supplemented with 20 ng ml^{-1} of epidermal growth factor (Sigma-Aldrich), 20 ng ml^{-1} of basic fibroblast growth factor (Sigma-Aldrich), B27 (1:50; Gibco) and penicillin–streptomycin (10,000 U ml^{-1} and 10,000 µg ml^{-1}; Gibco).

U138 (human glioblastoma) and U373 (human astrocytoma, grade III) cells were grown in modified Eagle's medium supplemented with 10% foetal calf serum (qualified, origin Australia), penicillin–streptomycin (10,000 U ml^{-1} and 10,000 µg ml^{-1}) and non-essential amino-acids (all from Gibco). Primary rat astrocytes were prepared as previously described (Etienne-Manneville, 2006). In non-confluent conditions, cell density was divided four times. For calcium depletion, primary rat astrocytes were cultured in Ca^{2+}-depleted medium (Gibco) supplemented with 0.5% foetal calf serum. In control conditions, Ca^{2+} (1.8 mM), glutaMAX and sodium pyruvate were added to the medium. JEG-3 epithelial cells were grown in minimum essential medium supplemented with 10% foetal calf serum, glutamax, nonessential amino acids and sodium pyruvate.

For wound-healing assays, primary rat astrocytes were seeded on coverslips coated with poly-L-ornithine (Sigma-Aldrich) or on Petri dishes and grown in the presence of serum to confluence. No coating was used for the two cell lines and primary glioblastomas. For all cell types, the medium was changed the day before scratching. Individual wounds were made with a cone tip (20–200 µl) or a blunt capillary. For biochemical analysis, multiple wounds were made with an eight-channel pipette (0.1–2 µl tips).

Live imaging experiments

Confluent cell monolayers were placed immediately after scratching in a Zeiss Axiovert 200M microscope, equipped with a humid chamber maintained at 37℃ with 5% CO_2 (10×, 0.45-NA objective and Hamamatsu ORCA II ER CCD camera) or an IncuCyte Live-Cell Imaging System (Essen BioScience, Ann Arbor, Michigan). We have used the IncuCyte FLR model that allows us to combine phase-contrast and fluorescence imaging for rescue experiments. Cell migration was recorded for 36 hours after the scratch. Movies were then analyzed using ImageJ software (W.S. Rasband, ImageJ, US National Institutes of Health, Bethesda, MD, http://rsb.info.nih.gov/ij/, 1997–2005). The manual tracking of the nucleus was used to follow migration of individual cells. In the rescue experiments, only GFP-positive cells were tracked and attention was paid not to include dying or suffering cells in the analysis. The average individual cell speeds were calculated from individual cell tracks by averaging the distances over the time interval from at least three independent experiments (Figs 2, 9) for the precise total number of cells in each cell culture condition. The persistence of migration is defined as the ratio between the vectorial distance (Dv), which is the real shifting of the cell, and the total distance (D) covered by the cell.

Immunofluorescence

We used the following antibodies or reagents: rat monoclonal anti-α-tubulin (1:100; Serotec, Kidlington, UK), rhodamin-coupled phalloidin (1:400; Molecular Probes, Invitrogen, Carlsbad, CA), rabbit polyclonal (1:200; Abcam, Cambridge, UK) or mouse monoclonal (diluted 1:100; BD Biosciences Transduction Laboratories, NJ,) anti-N-cadherin, mouse monoclonal anti-paxillin (1:100; BD Biosciences Transduction Laboratories), rabbit polyclonal anti-phospho-Src Y529 (1:100; Invitrogen), mouse monoclonal anti-GM130 (1:100; BD Biosciences Transduction Laboratories), rabbit polyclonal anti-pericentrin (1:200; Covance, Princeton, NJ, USA), rabbit polyclonal anti-βPIX (1:500; Chemicon, Billerica, MA), goat polyclonal anti-Par6 N-18 (1:50; Santa Cruz Biotechnology), rabbit polyclonal anti-PKCζ C-20 (1:100; Santa Cruz Biotechnology), and rabbit polyclonal antibodies against adenomatous polyposis coli (APC; gift from I. Näthke, University of Dundee, Dundee, UK). Donkey anti-mouse and donkey anti-rat coupled to CY2, donkey anti-rabbit TRITC and donkey anti-goat coupled to TRITC (1:200) were from Chemicon. Hoechst was used to visualize nuclei.

Cells were fixed in 4% paraformaldehyde in PBS, permeabilized in 0.2% Triton X-100 in PBS and blocked with sodium borohydride (0.5 mg ml^{-1}) in PBS (each for 10 minutes). Alternatively, for microtubule staining, cells were fixed in cold methanol for 5 minutes. Cells were then incubated for 1 hour with primary antibodies, washed three times in PBS and incubated another hour with secondary antibodies. Finally, coverslips were washed and mounted in Mowiol. Epifluorescence images were obtained on a microscope (model DM6000, Leica, Solms, Germany) equipped with 40×, NA 1.25 and a 63×, NA 1.4 objective lenses and were recorded on a CCD camera (CoolSNAP HQ, Roper Scientific, France) using Leica software. Grey-level images were treated and assembled using Adobe Photoshop and Adobe Illustrator CS2 software version 9.0 (Adobe System).

Western blotting

Cell lysates were obtained using Laemmli buffer containing 60 mM Tris-HCl pH 6.8, 10% glycerol, 2% SDS and 50 mM DTT. Proteins were analyzed by 10% SDS-PAGE and anti-N-cadherin (mouse monoclonal diluted 1:1000; BD Biosciences Transduction Laboratories), anti-pan-cadherin (mouse monoclonal, clone CH-19 diluted 1:1000, Sigma-Aldrich), rabbit polyclonal anti-phospho-Src Y529 (1:1000; Invitrogen) or mouse monoclonal anti-Src (clone L4A1, 1:1000; Cell Signaling Technology, Beverly, MA) western blotting. Anti-α-tubulin or anti-actin (mouse monoclonal; 1:4000, Sigma-Aldrich) western blotting was used as a control. Antibodies were diluted in PBS with 0.2% Tween and 4% milk, or TBS with 0.2% Tween and 4% milk and applied at room temperature. Washes were conducted with PBS with 0.2% Tween or TBS with 0.2% Tween. Quantification of signal intensity was performed using the ImageJ software and normalized to the control value. In the case of biopsy samples, quantification with the ODYSSEY Infrared Imaging system (LI-COR, Biosciences, Lincoln, NE) was used. Each N-cadherin signal was normalized with the β-actin signal intensity, using the Odyssey V3.0 software. The fluorescence signals were obtained using appropriate IRDye (LI-COR) infrared secondary antibodies.

DNA constructs and siRNAs

GFP–WT-Cdc42 was expressed by the pEGFP vector (Clontech Laboratories, Mountain View, CA). Nuclear microinjections were performed in the first row of wounded astrocytes in the first 30 minutes after scratching, and microinjected cells were returned to a 37℃, 5% CO_2 incubator. Expression vectors were used at 100–200 µg ml^{-1}. Protein expression was detectable ~1 hour after microinjection, and the cells were fixed 6–8 hours after microinjection.

pEGFP–N-cadherin was a gift of Cécile Gauthier-Rouvière (Mary et al., 2002). siRNA duplexes corresponding to rat N-cadherin were used as described previously (Dupin et al., 2009). pEGFP–N-cadherin (10–15 µg) and siRNA were introduced into cells using nucleofection technology (Amaxa, Cologne, Germany) as described previously (Etienne-Manneville et al., 2005). Transfected cells were fixed 4 days after nucleofection, and pEGFP–N-cadherin expression was detected with mouse monoclonal antibodies against GFP (diluted 1:100, Roche, France).

Measurements of polarity

Centrosome orientation

Centrosome reorientation in response to the scratch has already been characterized (Etienne-Manneville and Hall, 2001). This assay was performed 8 hours after wounding, and only the migrating astrocytes of the wounded edge were quantified. Centrosomes located in front of the nucleus, within the quadrant facing the wound, were scored as correctly oriented. A score of 25% represents the absolute minimum corresponding to random centrosome positioning. In rescue experiments, only the GFP-positive cells were taken into account.

Protein localization

To localize Cdc42 in cells, we microinjected the GFP–WT-Cdc42 construct (see above) because of the lack of anti-Cdc42 antibodies suitable for immunofluorescence. For βPIX, Par6 and PKCζ localization, cells were fixed 4 hours after wounding and stained with the appropriate antibodies. To quantify the protein recruitment, cells in which the protein was specifically enriched at the leading edge were scored as positive, as previously described (Osmani et al., 2006). Relative fluorescence intensity was measured at the leading edge using the ImageJ software, and graphs illustrate three representative cells for each considered protein. For this analysis, unmodified images were used.

APC recruitment at microtubule plus-ends was determined as described previously (Etienne-Manneville and Hall, 2003; Etienne-Manneville et al., 2005; Osmani et al., 2006). Cells were fixed 6 hours after wounding and stained with antibodies against APC and α-tubulin. The number of cells presenting APC clusters at the microtubule tips was determined.

As previously described (Osmani et al., 2006), primary rat astrocytes are very flat cells and they rarely form membrane ruffling at the leading edge. However, in order to avoid an artifact from increased fluorescence due to membrane ruffling, ruffling cells were not included in the analysis. On the contrary, U138 are very thick cells that do not show a clear leading edge. As a result, protein recruitment was not evaluated in these cells.

Focal adhesion quantifications

Surface quantifications

The mean surface occupied by focal adhesions was measured after binarization and thresholding of paxillin immunofluorescence grey-level acquisitions using the ImageJ software. Under non-confluent conditions, average cell surfaces were determined after manual drawing of individual cell outlines.

Number of focal adhesions

The average number of focal adhesions was calculated using the Anlayze Particles tool in ImageJ. Pixel size was chosen so as to include mature focal adhesions as well as most focal contacts. Under non-confluent conditions, the number of focal adhesions was determined in each cell. After the scratch, in confluent conditions, it was only quantified at the wound edges along the scratch, contained in a rectangle of 25 μm^2 surface area in order to avoid the cytoplasmic paxillin immunofluorescence observed in the perinuclear region, especially in glioma cells.

Cdc42 activity

GTP-bound Cdc42 was affinity purified using GST–PAK–PBD protein agarose beads and Cdc42 activation assay Biochem Kit (Cytoskeleton, Denver, CO). Proteins were analyzed by 15% SDS-PAGE and anti-Cdc42 western blotting using a specific mouse monoclonal antibody included in the kit (Cytoskeleton).

Statistical analysis

Statistical analysis was performed using GraphPad Prism 5.0. All data are presented as the mean ± s.e.m. One-way ANOVA analysis of the variance was followed by the Tukey's multiple comparison post-hoc test. Unpaired Student *t*-tests were used for LI-COR western blot quantification (Fig. 1B) and comparison of the average number of focal adhesions along the scratch (Fig. 4D). A P value of <0.05 was considered as statistically significant.

Acknowledgements

We are particularly grateful to Olivier Renaud from the Plate-Forme d'Imagerie Dynamique of Institut Pasteur, for his help with live-cell imaging. We thank Cécile Gauthier-Rouvière for the pEGFP–N-cadherin construct, Inke Nâthke for the gift of anti-APC antibodies and Matteo Bonazzi for JEG-3 cell cultures.

Funding

Funded by Institut National du Cancer [grant number 2009-1-RT-05 to E.C.]; the Association pour la Recherche sur le Cancer to N.O.; and the Ministère de l'enseignement supérieur et de la recherché to F.P. This work was also supported by the Centre National de la Recherche Scientifique; the Institut Pasteur; Association pour la Recherche sur le Cancer, La Ligue contre le Cancer. S.E.M. is a member of the EMBO YIP.

Supplementary material available online at
http://jcs.biologists.org/lookup/suppl/doi:10.1242/jcs.087668/-/DC1

References

Agiostratidou, G., Hulit, J., Phillips, G. R. and Hazan, R. B. (2007). Differential cadherin expression: potential markers for epithelial to mesenchymal transformation during tumor progression. *J. Mammary Gland Biol. Neoplasia* **12**, 127-133.

Amoureux, M. C., Coulibaly, B., Chinot, O., Loundou, A., Metellus, P., Rougon, G. and Figarella-Branger, D. (2010). Polysialic acid neural cell adhesion molecule (PSA-NCAM) is an adverse prognosis factor in glioblastoma, and regulates olig2 expression in glioma cell lines. *BMC Cancer* **10**, 91.

Andersson, A. M., Moran, N., Gaardsvoll, H., Linnemann, D., Bjerkvig, R., Laerum, O. D. and Bock, E. (1991). Characterization of NCAM expression and function in BT4C and BT4Cn glioma cells. *Int. J. Cancer* **47**, 124-129.

Angst, B. D., Marcozzi, C. and Magee, A. I. (2001). The cadherin superfamily: diversity in form and function. *J. Cell Sci.* **114**, 629-641.

Asano, K., Kubo, O., Tajika, Y., Huang, M. C., Takakura, K., Ebina, K. and Suzuki, S. (1997). Expression and role of cadherins in astrocytic tumors. *Brain Tumor Pathol.* **14**, 27-33.

Asano, K., Kubo, O., Tajika, Y., Takakura, K. and Suzuki, S. (2000). Expression of cadherin and CSF dissemination in malignant astrocytic tumors. *Neurosurg. Rev.* **23**, 39-44.

Asano, K., Duntsch, C. D., Zhou, Q., Weimar, J. D., Bordelon, D., Robertson, J. H. and Pourmotabbed, T. (2004). Correlation of N-cadherin expression in high grade gliomas with tissue invasion. *J. Neurooncol.* **70**, 3-15.

Borghi, N., Lowndes, M., Maruthamuthu, V., Gardel, M. L. and Nelson, W. J. (2010). Regulation of cell motile behavior by crosstalk between cadherin- and integrin-mediated adhesions. *Proc. Natl. Acad. Sci. USA* **107**, 13324-13329.

Cau, J. and Hall, A. (2005). Cdc42 controls the polarity of the actin and microtubule cytoskeletons through two distinct signal transduction pathways. *J. Cell Sci.* **118**, 2579-2587.

Desai, R. A., Gao, L., Raghavan, S., Liu, W. F. and Chen, C. S. (2009). Cell polarity triggered by cell–cell adhesion via E-cadherin. *J. Cell Sci.* **122**, 905-911.

Duenisch, P., Reichart, R., Mueller, U., Brodhun, M., Bjerkvig, R., Romeike, B., Walter, J., Herbold, C., Regenbrecht, C. R., Kalff, R. et al. (2010). Neural cell adhesion molecule isoform 140 declines with rise of WHO grade in human gliomas and serves as indicator for the invasion zone of multiform glioblastomas and brain metastases. *J. Cancer Res. Clin. Oncol.* **137**, 399-414.

Dupin, I., Camand, E. and Etienne-Manneville, S. (2009). Classical cadherins control nucleus and centrosome position and cell polarity. *J. Cell Biol.* **185**, 779-786.

Edvardsen, K., Pedersen, P. H., Bjerkvig, R., Hermann, G. G., Zeuthen, J., Laerum, O. D., Walsh, F. S. and Bock, E. (1994). Transfection of glioma cells with the neural-cell adhesion molecule NCAM: effect on glioma-cell invasion and growth in vivo. *Int. J. Cancer* **58**, 116-122.

Etienne-Manneville, S. (2004). Cdc42 – the centre of polarity. *J. Cell Sci.* **117**, 1291-1300.

Etienne-Manneville, S. (2006). In vitro assay of primary astrocyte migration as a tool to study Rho GTPase function in cell polarization. *Methods Enzymol.* **406**, 565-578.

Etienne-Manneville, S. and Hall, A. (2001). Integrin-mediated activation of Cdc42 controls cell polarity in migrating astrocytes through PKCzeta. *Cell* **106**, 489-498.

Etienne-Manneville, S. and Hall, A. (2003). Cdc42 regulates GSK-3beta and adenomatous polyposis coli to control cell polarity. *Nature* **421**, 753-756.

Etienne-Manneville, S., Manneville, J. B., Nicholls, S., Ferenczi, M. A. and Hall, A. (2005). Cdc42 and Par6-PKCzeta regulate the spatially localized association of Dlg1 and APC to control cell polarization. *J. Cell Biol.* **170**, 895-901.

Faber-Elman, A., Solomon, A., Abraham, J. A., Marikovsky, M. and Schwartz, M. (1996). Involvement of wound-associated factors in rat brain astrocyte migratory response to axonal injury: in vitro simulation. *J. Clin. Invest.* **97**, 162-171.

Feng, Q., Baird, D. and Cerione, R. A. (2004). Novel regulatory mechanisms for the Dbl family guanine nucleotide exchange factor Cool-2/alpha-Pix. *EMBO J.* **23**, 3492-3504.

Feng, Q., Baird, D., Yoo, S., Antonyak, M. and Cerione, R. A. (2010). Phosphorylation of the cool-1/beta-Pix protein serves as a regulatory signal for the migration and invasive activity of Src-transformed cells. *J. Biol. Chem.* **285**, 18806-18816.

Foty, R. A. and Steinberg, M. S. (2004). Cadherin-mediated cell–cell adhesion and tissue segregation in relation to malignancy. *Int. J. Dev. Biol.* **48**, 397-409.

Frame, M. C. and Brunton, V. G. (2002). Advances in Rho-dependent actin regulation and oncogenic transformation. *Curr. Opin. Genet. Dev.* **12**, 36-43.

Frank, S. R. and Hansen, S. H. (2008). The PIX–GIT complex: a G protein signaling cassette in control of cell shape. *Semin. Cell Dev. Biol.* **19**, 234-244.

Giese, A. (2003). Glioma invasion – pattern of dissemination by mechanisms of invasion and surgical intervention, pattern of gene expression and its regulatory control by tumorsuppressor p53 and proto-oncogene ETS-1. *Acta Neurochir. Suppl.* **88**, 153-162.

Gimond, C., van Der Flier, A., van Delft, S., Brakebusch, C., Kuikman, I., Collard, J. G., Fassler, R. and Sonnenberg, A. (1999). Induction of cell scattering by expression of beta1 integrins in beta1-deficient epithelial cells requires activation of members of the rho family of GTPases and downregulation of cadherin and catenin function. *J. Cell Biol.* **147**, 1325-1340.

Gratsa, A., Rooprai, H. K., Rogers, J. P., Martin, K. K. and Pilkington, G. J. (1997). Correlation of expression of NCAM and GD3 ganglioside to motile behaviour in neoplastic glia. *Anticancer Res.* **17**, 4111-4117.

Guarino, M. (2010). Src signaling in cancer invasion. *J. Cell Physiol.* **223**, 14-26.

Gupton, S. L., Eisenmann, K., Alberts, A. S. and Waterman-Storer, C. M. (2007). mDia2 regulates actin and focal adhesion dynamics and organization in the lamella for efficient epithelial cell migration. *J. Cell Sci.* **120**, 3475-3487.

Hall, A. (2005). Rho GTPases and the control of cell behaviour. *Biochem. Soc. Trans.* **33**, 891-895.

Hatta, K. and Takeichi, M. (1986). Expression of N-cadherin adhesion molecules associated with early morphogenetic events in chick development. *Nature* **320**, 447-449.

Hazan, R. B., Qiao, R., Keren, R., Badano, I. and Suyama, K. (2004). Cadherin switch in tumor progression. *Ann. New York Acad. Sci.* **1014**, 155-163.

Hegedus, B., Marga, F., Jakab, K., Sharpe-Timms, K. L. and Forgacs, G. (2006). The interplay of cell–cell and cell–matrix interactions in the invasive properties of brain tumors. *Biophys. J.* **91**, 2708-2716.

Humbert, P., Russell, S. and Richardson, H. (2003). Dlg, Scribble and Lgl in cell polarity, cell proliferation and cancer. *BioEssays* **25**, 542-553.

Huttenlocher, A., Lakonishok, M., Kinder, M., Wu, S., Truong, T., Knudsen, K. A. and Horwitz, A. F. (1998). Integrin and cadherin synergy regulates contact inhibition of migration and motile activity. *J. Cell Biol.* **141**, 515-526.

Iden, S. and Collard, J. G. (2008). Crosstalk between small GTPases and polarity proteins in cell polarization. *Nat. Rev. Mol. Cell Biol.* **9**, 846-859.

Izumi, Y., Hirose, T., Tamai, Y., Hirai, S., Nagashima, Y., Fujimoto, T., Tabuse, Y., Kemphues, K. J. and Ohno, S. (1998). An atypical PKC directly associates and colocalizes at the epithelial tight junction with ASIP, a mammalian homologue of *Caenorhabditis elegans* polarity protein PAR-3. *J. Cell Biol.* **143**, 95-106.

Jung, T. Y., Jung, S., Lee, K. H., Cao, V. T., Jin, S. G., Moon, K. S., Kim, I. Y., Kang, S. S., Kim, H. S. and Lee, M. C. (2010). Nogo-A expression in oligodendroglial tumors. *Neuropathology* **31**, 11-19.

Kang, Y. and Massague, J. (2004). Epithelial–mesenchymal transitions: twist in development and metastasis. *Cell* **118**, 277-279.

Kleihues, P., Burger, P. C. and Scheithauer, B. W. (1993). The new WHO classification of brain tumours. *Brain Pathol.* **3**, 255-268.

Kohutek, Z. A., diPierro, C. G., Redpath, G. T. and Hussaini, I. M. (2009). ADAM-10-mediated N-cadherin cleavage is protein kinase C-alpha dependent and promotes glioblastoma cell migration. *J. Neurosci.* **29**, 4605-4615.

Kuphal, S. and Bosserhoff, A. K. (2006). Influence of the cytoplasmic domain of E-cadherin on endogenous N-cadherin expression in malignant melanoma. *Oncogene* **25**, 248-259.

Lewis-Tuffin, L. J., Rodriguez, F., Giannini, C., Scheithauer, B., Necela, B. M., Sarkaria, J. N. and Anastasiadis, P. Z. (2010). Misregulated E-cadherin expression associated with an aggressive brain tumor phenotype. *PLoS ONE* **5**, e13665.

Louis, D. N., Ohgaki, H., Wiestler, O. D., Cavenee, W. K., Burger, P. C., Jouvet, A., Scheithauer, B. W. and Kleihues, P. (2007). The 2007 WHO classification of tumours of the central nervous system. *Acta Neuropathol.* **114**, 97-109.

Maeda, M., Johnson, K. R. and Wheelock, M. J. (2005). Cadherin switching: essential for behavioral but not morphological changes during an epithelium–to–mesenchyme transition. *J. Cell Sci.* **118**, 873-887.

Maidment, S. L., Rucklidge, G. J., Rooprai, H. K. and Pilkington, G. J. (1997). An inverse correlation between expression of NCAM-A and the matrix-metalloproteinases gelatinase-A and gelatinase-B in human glioma cells in vitro. *Cancer Lett.* **116**, 71-77.

Makrilia, N., Kollias, A., Manolopoulos, L. and Syrigos, K. (2009). Cell adhesion molecules: role and clinical significance in cancer. *Cancer Invest.* **27**, 1023-1037.

Manabe, N., Hirai, S., Imai, F., Nakanishi, H., Takai, Y. and Ohno, S. (2002). Association of ASIP/mPAR-3 with adherens junctions of mouse neuroepithelial cells. *Dev. Dyn.* **225**, 61-69.

Mary, S., Charrasse, S., Meriane, M., Comunale, F., Travo, P., Blangy, A. and Gauthier-Rouviere, C. (2002). Biogenesis of N-cadherin-dependent cell–cell contacts in living fibroblasts is a microtubule-dependent kinesin-driven mechanism. *Mol. Biol. Cell* **13**, 285-301.

McLendon, R., Friedman, A., Bigner, D., Van Meir, E. G., Brat, D. J., Mastrogianakis, G. M., Olson, J. J., Mikkelsen, T., Lehman, N., Aldape, K. et al. (2008). Comprehensive genomic characterization defines human glioblastoma genes and core pathways. *Nature* **455**, 1061-1068.

Micalizzi, D. S., Farabaugh, S. M. and Ford, H. L. (2010). Epithelial–mesenchymal transition in cancer: parallels between normal development and tumor progression. *J. Mammary Gland Biol. Neoplasia* **15**, 117-134.

Michaelson, D., Silletti, J., Murphy, G., D'Eustachio, P., Rush, M. and Philips, M. R. (2001). Differential localization of Rho GTPases in live cells: regulation by hypervariable regions and RhoGDI binding. *J. Cell Biol.* **152**, 111-126.

Nakajima, S., Doi, R., Toyoda, E., Tsuji, S., Wada, M., Koizumi, M., Tulachan, S. S., Ito, D., Kami, K., Mori, T. et al. (2004). N-cadherin expression and epithelial–mesenchymal transition in pancreatic carcinoma. *Clin. Cancer Res.* **10**, 4125-4133.

Nishiyama, A., Onda, K., Washiyama, K., Kumanishi, T., Kuwano, R., Sakimura, K. and Takahashi, Y. (1989). Differential expression of glial fibrillary acidic protein in human glioma cell lines. *Acta Neuropathol.* **78**, 9-15.

Nobes, C. D. and Hall, A. (1999). Rho GTPases control polarity, protrusion, and adhesion during cell movement. *J. Cell Biol.* **144**, 1235-1244.

Osmani, N., Vitale, N., Borg, J. P. and Etienne-Manneville, S. (2006). Scrib controls Cdc42 localization and activity to promote cell polarization during astrocyte migration. *Curr. Biol.* **16**, 2395-2405.

Osmani, N., Peglion, F., Chavrier, P. and Etienne-Manneville, S. (2010). Cdc42 localization and cell polarity depend on membrane traffic. *J. Cell Biol.* **191**, 1261-1269.

Owens, G. C., Orr, E. A., DeMasters, B. K., Muschel, R. J., Berens, M. E. and Kruse, C. A. (1998). Overexpression of a transmembrane isoform of neural cell adhesion molecule alters the invasiveness of rat CNS-1 glioma. *Cancer Res.* **58**, 2020-2028.

Peng, H., Shah, W., Holland, P. and Carbonetto, S. (2008). Integrins and dystroglycan regulate astrocyte wound healing: the integrin beta1 subunit is necessary for process extension and orienting the microtubular network. *Dev. Neurobiol.* **68**, 559-574.

Pera, I. L., Iuliano, R., Florio, T., Susini, C., Trapasso, F., Santoro, M., Chiariotti, L., Schettini, G., Viglietto, G. and Fusco, A. (2005). The rat tyrosine phosphatase eta increases cell adhesion by activating c-Src through dephosphorylation of its inhibitory phosphotyrosine residue. *Oncogene* **24**, 3187-3195.

Perego, C., Vanoni, C., Massari, S., Raimondi, A., Pola, S., Cattaneo, M. G., Francolini, M., Vicentini, L. M. and Pietrini, G. (2002). Invasive behaviour of glioblastoma cell lines is associated with altered organisation of the cadherin–catenin adhesion system. *J. Cell Sci.* **115**, 3331-3340.

Ponten, J. and Macintyre, E. H. (1968). Long term culture of normal and neoplastic human glia. *Acta Pathol. Microbiol. Scand.* **74**, 465-486.

Prestegarden, L., Svendsen, A., Wang, J., Sleire, L., Skaftnesmo, K. O., Bjerkvig, R., Yan, T., Askland, L., Persson, A., Sakariassen, P. O. et al. (2010). Glioma cell populations grouped by different cell type markers drive brain tumor growth. *Cancer Res.* **70**, 4274-4279.

Raftopoulou, M., Etienne-Manneville, S., Self, A., Nicholls, S. and Hall, A. (2004). Regulation of cell migration by the C2 domain of the tumor suppressor PTEN. *Science* **303**, 1179-1181.

Rappl, A., Piontek, G. and Schlegel, J. (2008). EGFR-dependent migration of glial cells is mediated by reorganisation of N-cadherin. *J. Cell Sci.* **121**, 4089-4097.

Reynolds, A. B. and Carnahan, R. H. (2004). Regulation of cadherin stability and turnover by p120ctn: implications in disease and cancer. *Semin. Cell Dev. Biol.* **15**, 657-663.

Sabatini, P. J., Zhang, M., Silverman-Gavrila, R., Bendeck, M. P. and Langille, B. L. (2008). Homotypic and endothelial cell adhesions via N-cadherin determine polarity and regulate migration of vascular smooth muscle cells. *Circ. Res.* **103**, 405-412.

Shen, Y., Li, N., Wu, S., Zhou, Y., Shan, Y., Zhang, Q., Ding, C., Yuan, Q., Zhao, F., Zeng, R. et al. (2008). Nudel binds Cdc42GAP to modulate Cdc42 activity at the leading edge of migrating cells. *Dev. Cell* **14**, 342-353.

Shinoura, N., Paradies, N. E., Warnick, R. E., Chen, H., Larson, J. J., Tew, J. J., Simon, M., Lynch, R. A., Kanai, Y., Hirohashi, S. et al. (1995). Expression of N-cadherin and alpha-catenin in astrocytomas and glioblastomas. *Br. J. Cancer* **72**, 627-633.

Suzuki, M., Nakayama, J., Suzuki, A., Angata, K., Chen, S., Sakai, K., Hagihara, K., Yamaguchi, Y. and Fukuda, M. (2005). Polysialic acid facilitates tumor invasion by glioma cells. *Glycobiology* **15**, 887-894.

Takeichi, M. (1990). Cadherins: a molecular family important in selective cell–cell adhesion. *Annu. Rev. Biochem.* **59**, 237-252.

Thiery, J. P. (2002). Epithelial–mesenchymal transitions in tumour progression. *Nat. Rev. Cancer* **2**, 442-454.

Utsuki, S., Sato, Y., Oka, H., Tsuchiya, B., Suzuki, S. and Fujii, K. (2002). Relationship between the expression of E-, N-cadherins and beta-catenin and tumor grade in astrocytomas. *J. Neurooncol.* **57**, 187-192.

Vega, F. M. and Ridley, A. J. (2008). Rho GTPases in cancer cell biology. *FEBS Lett.* **582**, 2093-3101.

Vielreicher, M., Harms, G., Butt, E., Walter, U. and Obergfell, A. (2007). Dynamic interaction between Src and C-terminal Src kinase in integrin alphaIIbbeta3-mediated signaling to the cytoskeleton. *J. Biol. Chem.* **282**, 33623-33631.

Watanabe, T., Noritake, J. and Kaibuchi, K. (2005). Regulation of microtubules in cell migration. *Trends Cell Biol.* **15**, 76-83.

Xiao, K., Oas, R. G., Chiasson, C. M. and Kowalczyk, A. P. (2007). Role of p120-catenin in cadherin trafficking. *Biochim. Biophys. Acta* **1773**, 8-16.

Yano, H., Mazaki, Y., Kurokawa, K., Hanks, S. K., Matsuda, M. and Sabe, H. (2004). Roles played by a subset of integrin signaling molecules in cadherin-based cell-cell adhesion. *J. Cell Biol.* **166**, 283-295.